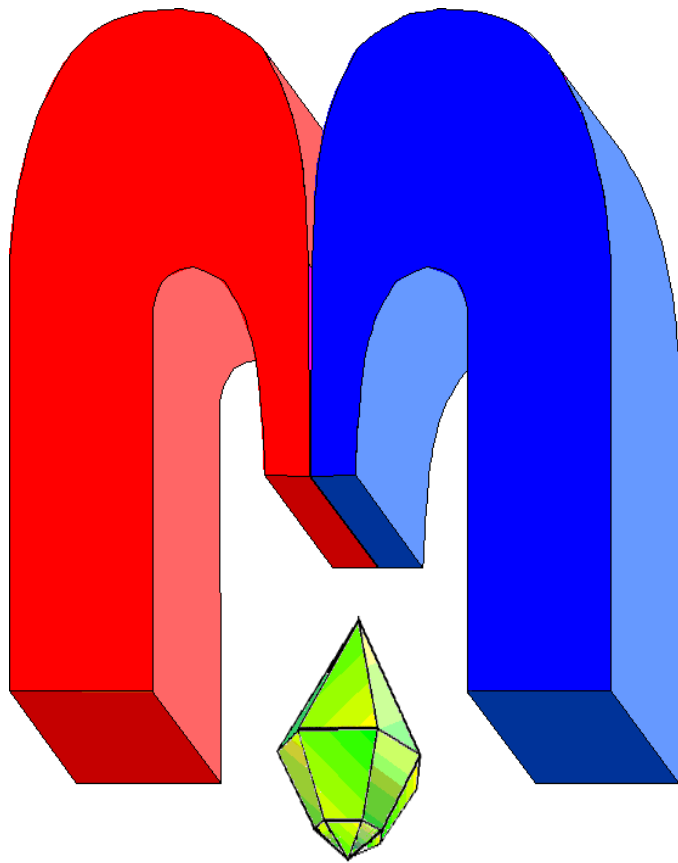


ISSN 2072-5981
doi: 10.26907/mrsej



***magnetic
Resonance
in Solids***

Electronic Journal

Volume 26

Issue 2

Article No 24218

1-7 pages

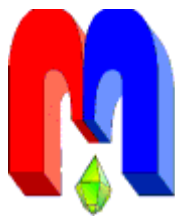
June, 6

2024

doi: 10.26907/mrsej-24218

<http://mrsej.kpfu.ru>

<https://mrsej.elpub.ru>



Established and published by Kazan University*
Endorsed by International Society of Magnetic Resonance (ISMAR)
Registered by Russian Federation Committee on Press (#015140),
August 2, 1996
First Issue appeared on July 25, 1997

© Kazan Federal University (KFU)†

"Magnetic Resonance in Solids. Electronic Journal" (MRSej) is a peer-reviewed, all electronic journal, publishing articles which meet the highest standards of scientific quality in the field of basic research of a magnetic resonance in solids and related phenomena.

Indexed and abstracted by
Web of Science (ESCI, Clarivate Analytics, from 2015), Scopus (Elsevier, from 2012), RusIndexSC (eLibrary, from 2006), Google Scholar, DOAJ, ROAD, CyberLeninka (from 2006), SCImago Journal & Country Rank, etc.

Editor-in-Chief

Boris **Kochelaev** (KFU, Kazan)

Honorary Editors

Jean **Jeener** (Universite Libre de Bruxelles, Brussels)

Raymond **Orbach** (University of California, Riverside)


Executive Editor

Yurii **Proshin** (KFU, Kazan)

mrsej@kpfu.ru



This work is licensed under a [Creative Commons Attribution-ShareAlike 4.0 International License](https://creativecommons.org/licenses/by-sa/4.0/).

 This is an open access journal which means that all content is freely available without charge to the user or his/her institution. This is in accordance with the [BOAI definition of open access](https://www.boai.ru/).

Technical Editors

Maxim **Avdeev** (KFU, Kazan)
Vadim **Tumanov** (KFU, Kazan)
Fail **Sirayev** (KFU, Kazan)

Editors

Vadim **Atsarkin** (Institute of Radio Engineering and Electronics, Moscow)

Yurij **Bunkov** (CNRS, Grenoble)

Mikhail **Eremin** (KFU, Kazan)

David **Fushman** (University of Maryland, College Park)

Hugo **Keller** (University of Zürich, Zürich)

Yoshio **Kitaoka** (Osaka University, Osaka)

Boris **Malkin** (KFU, Kazan)

Alexander **Shengelaya** (Tbilisi State University, Tbilisi)

Jörg **Sichelschmidt** (Max Planck Institute for Chemical Physics of Solids, Dresden)

Haruhiko **Suzuki** (Kanazawa University, Kanazawa)

Murat **Tagirov** (KFU, Kazan)

Dmitrii **Tayurskii** (KFU, Kazan)

Valentine **Zhikharev** (KNRTU, Kazan)

Invited Editor of Special Issue[‡]: Eduard Baibekov (KFU, Kazan)

* Address: "Magnetic Resonance in Solids. Electronic Journal", Kazan Federal University; Kremlevskaya str., 18; Kazan 420008, Russia

† In Kazan University the Electron Paramagnetic Resonance (EPR) was discovered by Zavoisky E.K. in 1944.

‡ Dedicated to Professor Boris Z. Malkin on the occasion of his 85th birthday

Broadening of the silicon vacancy EPR line in SiC revealed through optically selective excitation[†]

B. V. Yavkin¹, V. A. Soltamov², F. F. Murzakhanov³,
G. V. Mamin³, E. N. Mokhov², E. Goovaerts⁴

¹CEA, SPEC, Gif-sur-Yvette 91191, France

²Ioffe Institute, St. Petersburg 194021, Russia

³Kazan Federal University, Kazan 420008, Russia

⁴University of Antwerp, Wilrijk 2610, Belgium

*E-mail: *boris.yavkin@gmail.com*

(Received May 9, 2024; accepted May 30, 2024; published June 6, 2024)

In SiC crystal enriched by ²⁸Si isotope with nuclear spin $I = 0$, two negatively charged silicon vacancy centers V_{Si}^- , V_{k1} and V_{k2} were investigated using X-band CW electron paramagnetic resonance (EPR) spectroscopy combined with tunable Ti-sapphire laser excitation. For the V_{k1} and V_{k2} centers, the EPR line position depends on the optical excitation energy which demonstrates inhomogeneous broadening of the optical transition correlated with variations in the zero field splitting.

PACS: 76.30.-v, 61.72.Hh, 61.72.J-, 76.30.Mi, 61.72-y, 78.55.Et, 71.55.Gs

Keywords: electron paramagnetic resonance, photoluminescence, resonant optical excitation, silicon carbide, silicon vacancy

1. Introduction

SiC crystals are considered as host materials for a number of solid-state defects with peculiar properties [1–3]. Many of the defects are optically active in visible and infrared regions, and some have coupled spin-optical properties like spin-dependent photoluminescence [4–6]. Among the plethora of possible applications, sensors and nodes of quantum information processing networks are among the most intriguing [3,4,7]. Detailed understanding and control of the properties of the crystal and of defects appearing in it [8]], are of the utmost importance for further development towards practical applications. Electron paramagnetic resonance (EPR) being one of the most informative method to elucidate the structure, symmetry and spin properties of local defects, was effectively applied to the case of various paramagnetic defects in silicon carbide, and in particular to Si vacancies [9,10]. In this work, selective optical excitation and conventional EPR are brought together to address the question of spectroscopic parameter distribution over the ensemble of V_{Si}^- defects beyond the unresolved inhomogeneous linewidth.

2. Materials and Methods

2.1. SiC crystal

A silicon carbide crystal 6H-²⁸SiC was grown by the physical vapor transport method [11, 12] using an isotopically-enriched silicon precursor and single-crystal 6H-SiC substrate with natural isotope content of ²⁹Si ($I = 1/2$, 4.7%) and ¹³C ($I = 1/2$, 1.1%) as a growth seed. The concentration of the ²⁹Si isotope in the grown crystal was estimated at 1% [13]. To create V_{Si}^- centers, crystal was irradiated by electrons with 2 MeV energy and 10^{18} cm⁻² dose, and subsequently annealed for 30 minutes in Ar atmosphere.

[†]This paper is dedicated to Professor Boris Z. Malkin, who made a significant contribution to the field of magnetic radio spectroscopy in Kazan University, on the occasion of his 85th birthday.

2.2. EPR with wavelength-tunable laser excitation

A commercial X-band (9.6 GHz) Bruker E580II EPR spectrometer was used.

The standard sample holder was modified to accommodate the SiC crystal and optical fiber. Optical excitation source was Newport Ti-Sapphire laser equipped with OPO. The laser wavelength was tunable in the range 850–950 nm and accurately checked with the wavemeter with the precision of 0.02 nm, laser spectral linewidth was approx. 40 GHz. Laser light was coupled to 125 μm thick fiber core by a system of mirrors and coupler and guided in the fiber to the sample continuously.

All EPR measurements were performed at the temperature of 10 K, cooling was provided by Oxford Instruments helium flow cryostat. To prevent laser induced sample heating, a low power level of ≈ 2 mW at the entrance of the fiber coupler was used.

3. Results and Discussion

In 6H-SiC lattice three non-equivalent Si sites exist (two quasi-cubic and one quasi-hexagonal) [14], hence there are three non-equivalent negatively charged silicon vacancy V_{Si}^- centers. These point defects have been identified optically and are distinguished by their respective zero-phonon lines (ZPL) as V1 (865 nm), V2 (887 nm) and V3 (905 nm). Additionally, their presence have been confirmed by EPR spectroscopy, which reveals characteristic orientation dependence of the splitting between spin resonance lines, indicating axially symmetric high spin centers ($S = 3/2$). The corresponding splitting reaches its maximal value when the static magnetic field \mathbf{B} oriented parallel to crystal c -axis. At this orientation each pair of EPR signals attributed to the fine structure of V_{Si}^- defects is characterized by the following splittings: V_h (≈ 0 Gauss), V_{k2} (≈ 91 Gauss) and V_{k1} (≈ 20 Gauss), enumerated according to the ZPL list above [4, 15–17]. The ground state of V_{Si}^- defects can be described by the following Hamiltonian:

$$H = g\beta S_z B_0 + D[S_z^2 - S(S+1)/3], \quad (1)$$

where $g \approx 2.003$ is typical gyromagnetic factor of the V_{Si}^- defect family, and D is axial zero-field splitting parameter. The difference in resonance fields between low- and high-field transition or the splitting in EPR spectrum (see Fig. 1) is $4D$ (sample orientation in external magnetic field is c -axis parallel to the field throughout the text). At non-resonant optical excitation ($\lambda \approx 860$ nm), the EPR spectrum shows a typical picture of central line at $g \approx 2$, and two pairs of lines splitted by 9190.8 G and 19.2 G, attributed to V_{k2} and V_{k1} . The signal from the third one, the V_h defect, is located at the center of spectrum and is poorly separable from the other paramagnetic centers at $g = 2$. It is worth noting that the linewidth of transitions is particularly small ≈ 0.3 G due to diluted nuclear spin environment which allows for resolvable splitting of ≈ 2.8 G caused by the hyperfine interaction with ^{29}Si nuclear spins in second coordination shell of Si site visible at the shoulders of main transitions [18].

The phase reversal between low and high field transition is due to laser induced hyperpolarization of the $M_S = \pm 3/2$ spin sublevels [19].

In the following experiments, the detailed observation of laser-induced changes in the EPR lines will be addressed using resonant optical excitation. High-resolution optical spectroscopy measurements performed elsewhere allowed us to target a specific laser wavelength to resonantly excite one or the other center. In the condition of near-resonant optical excitation at ZPL of V2 (or V_{k2}) its EPR line intensity and position were changing according to the wavelength sweep, as depicted in the Fig. 2 below. A similar effect was observed for excitation into ZPL of V3 (or

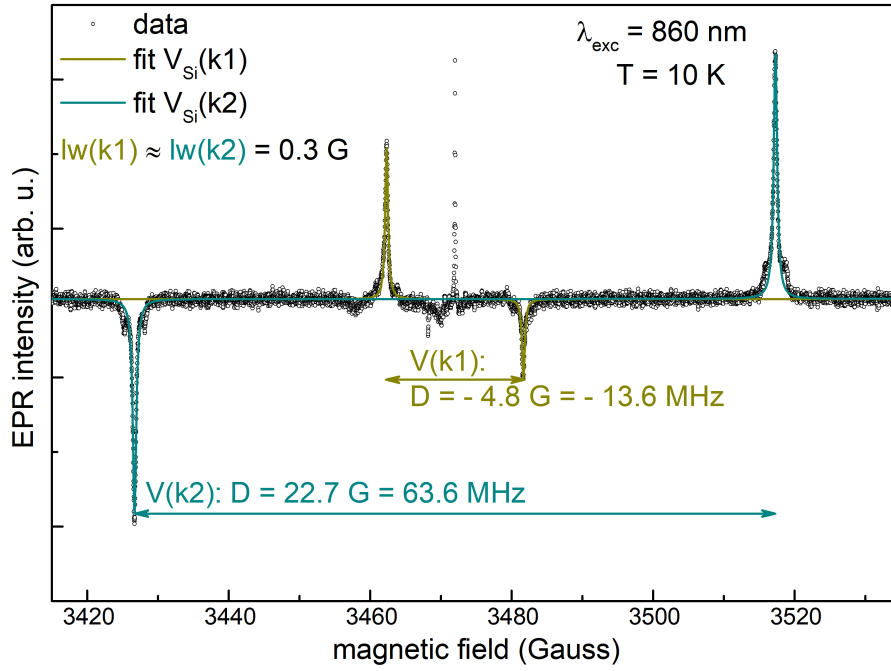


Figure 1. X-band ($f = 9.74$ GHz) EPR spectrum of SiC sample recorded at 10 K under non-resonant 860 nm laser excitation. V_{k1} and V_{k2} centers are identified by specific splitting between low- and high-field transitions, zero-field parameter D is derived from this splitting. Note that D is negative for V_{k1} .

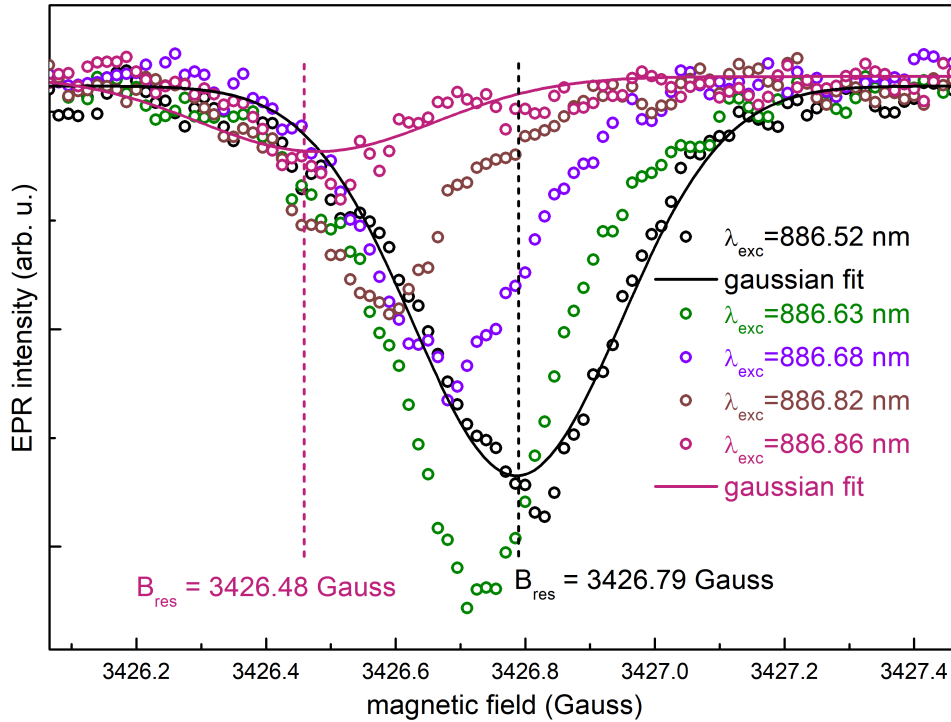


Figure 2. Resonance field shift and line intensity change of low-field V_{k2} transition while sweeping laser excitation around the optical resonance transition.

V_{k1}). In this work we focus on the shift in resonance field that we attributed to the variation in observed zero field splitting D . For the detailed study of high-resolution optical spectroscopy and light-induced changes in the intensity of EPR signal, the reader is referred to the work [5].

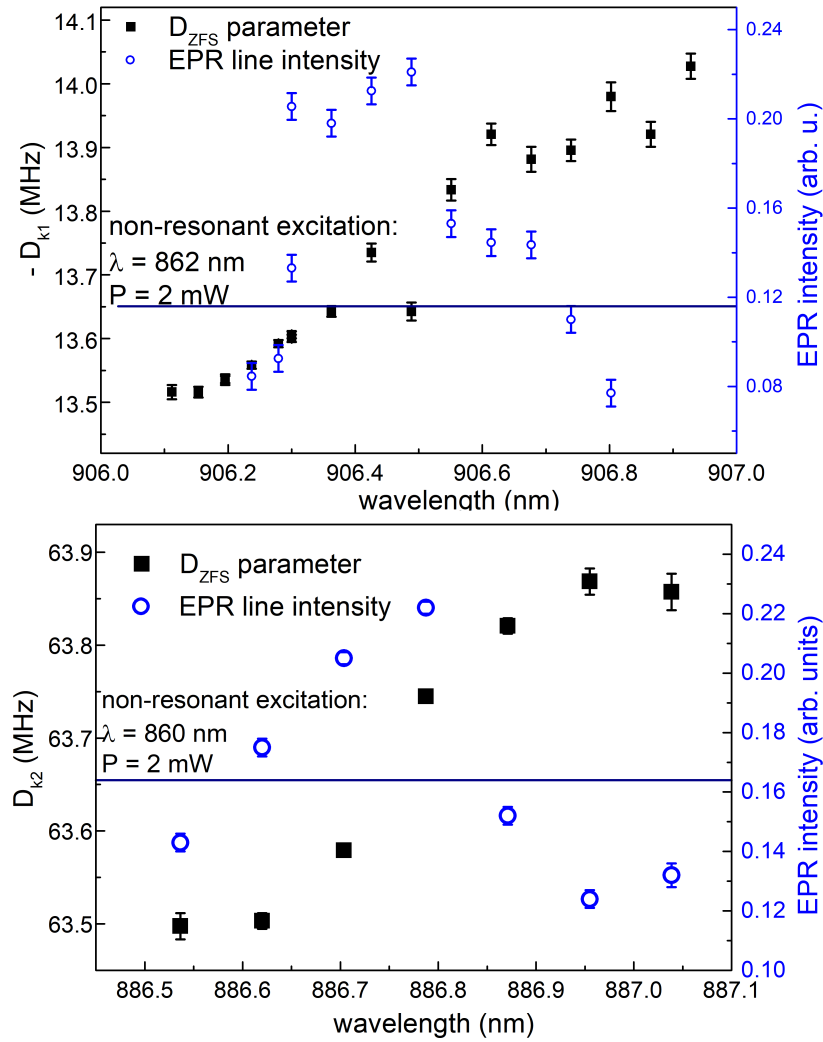


Figure 3. EPR intensity and zero-field splitting parameter D plotted vs excitation wavelength for (top) V_{k1} and (bottom) V_{k2} centers. Straight lines (non-resonant excitation) are indicating the value of D for excitation with laser sufficiently detuned from the optical transition of each center.

Both high- and low-field transitions were monitored and fitted together by Eq. 1 to distinguish changes in splitting between EPR lines from mere line shift. The changes in transition field values are minimal, only 0.3 G resonance field shift over 0.3 nm wavelength sweep, therefore special care was necessary to confirm the change in the line splitting. Combined experimental data on the changes in D and relative EPR line intensity plotted versus optical excitation are presented in Fig. 3 for two V_{k1} and V_{k2} centers. We note that sweeping the laser excitation near resonant optical transition allows addressing sub-ensembles of paramagnetic centers which are not accessible directly by optical excitation or by EPR alone. It is remarkable that the double-resonance technique employed here allows resolution of 100 kHz at the level of 40 GHz-width excitation. The following Figure 4 represents a reconstruction of the V_{k1} and V_{k2} ensembles by plotting normalized EPR intensity of transitions versus D , from which the characteristic width, or histogram of zero-field parameter distribution, is derived. It is interesting to note that ensemble distribution linewidth of V_{k1} is 3 times larger than for V_{k2} center. We suppose this difference is related to spin density distribution for both centers and suppose that needle-like configuration of V_{k1} [18] is more susceptible to the local strain, which causes larger ensemble broadening.

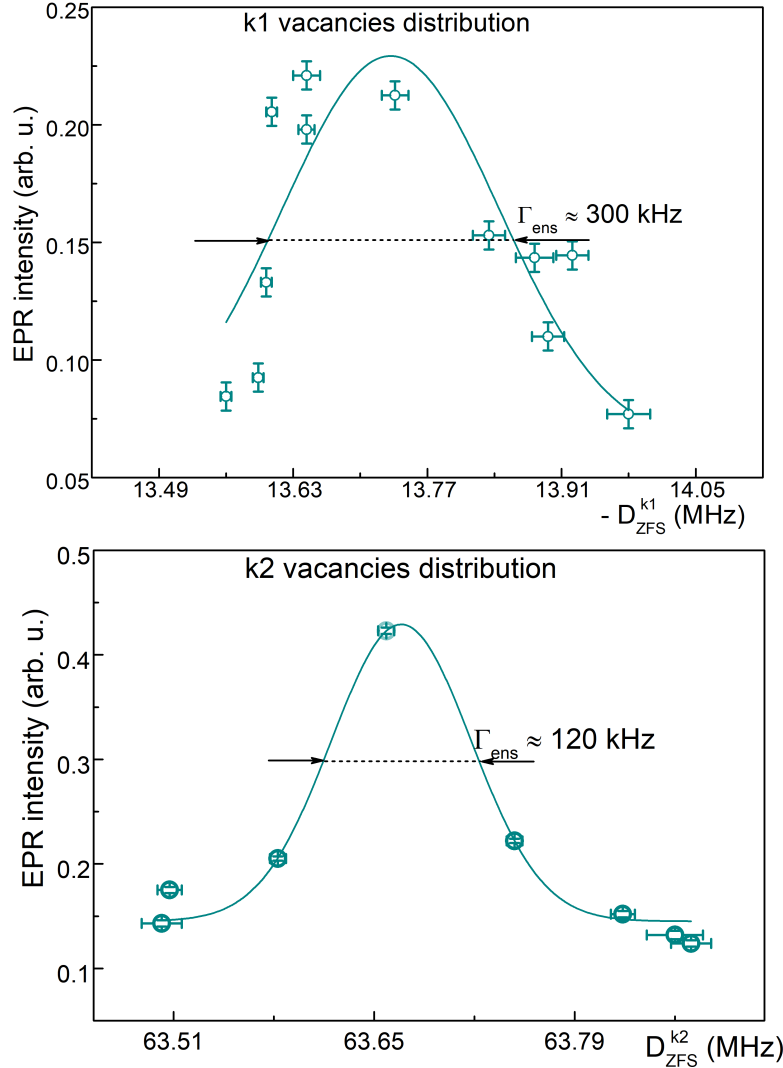


Figure 4. EPR intensity plotted over zero-field splitting parameter D for (top) V_{k1} and (bottom) V_{k2} centers. The solid line are gaussian fits allowed for estimation the width of the ensemble distribution.

4. Conclusion

We have studied a SiC crystal of 6H grown polytype in a ^{29}Si -depleted environment that allowed for narrow EPR transition of 0.3 G in linewidth and resolvable hyperfine splittings. We demonstrated selective subensemble excitation of V_{Si}^- centers and revealed correlation between inhomogenous broadening of the optical and EPR transition. A reduction of EPR linewidth is observed, namely, from ensemble-broadened value of ≈ 1 MHz (in case of non-resonant excitation) down to ≈ 100 kHz (in case of near-resonance one). Finally, it appears that further advance on the research initiated by this article will be interesting, towards the demonstration of excitation transfer between subensembles, and understanding of their spatial arrangement within the crystal, in a manner somewhat similar to reconstruction of nuclear spin environment in other solid-state defects [20].

Acknowledgments

The study was partially funded by the subsidy allocated to Kazan Federal University for the state assignment in the sphere of scientific activities (Project No. FZSM-2024-0010).

References

1. Atatuere M., Englund D., Vamivakas N., Lee S.-Y., Wrachtrup J., *Nature Rev. Mater.* **3**, 38 (2018).
2. Kraus H., Soltamov V. A., Fuchs F., Sperlich A., Baranov P. G., Astakhov G. V., Dyakonov V., *Sci. Rep.* **4**, 5303 (2014).
3. Awschalom D., Hanson R., Wrachtrup J., Zhou J., *Nature Photon.* **12**, 516 (2018).
4. Baranov P. G., Bundakova A. P., Soltamova A. A., Orlinskii S. B., Borovykh I. V., Zonder-van R., Verberk R., Schmidt J., *Phys. Rev. B* **83**, 125203 (2011).
5. Riedel D., Fuchs F., Kraus H., Vaeth S., Sperlich A., Dyakonov V., Soltamova A. A., Baranov P. G., Ilyin V. A., Astakhov G. V., *Phys. Rev. Lett.* **109**, 226402 (2012).
6. Koehl W. F., Buckley B. B., Heremans F. J., Calusine G., Awschalom D. D., *Nature* **479**, 84 (2011).
7. Castelletto S., Lew T. K., Lin W.-X., Xu J.-S., *Rep. Prog. Phys.* **87**, 014501 (2023).
8. Kimoto T., Cooper J. A., *Fundamentals of Silicon Carbide Technology: Growth, Characterization, Devices and Applications* (John Wiley and Sons, 2014) 400 p.
9. Vainer V. S., Il'in V. A., *Sov. Phys. Solid State* **23**, 2126 (1981).
10. Schneider J., Maier K., *Physica B* **185**, 199 (1993).
11. Heydemann V. D., Schulze N., Barrett D. L., Pensl G., *Appl. Phys. Lett.* **69**, 3728 (1996).
12. Mokhov E., Ramm M., Roenkov A., Vodakov Y., *Mater. Sci. Engin.: B* **46**, 317 (1997).
13. Soltamov V. A., Kasper C., Poshakinskiy A. V., Anisimov A. N., Mokhov E. N., Sperlich A., Tarasenko S. A., Baranov P. G., Astakhov G. V., Dyakonov V., *Nature Comm.* **10**, 1678 (2019).
14. Powell J. A., Pirouz P., Choyke W. J., "Growth and characterization of silicon carbide polytypes for electronic applications," in *Semiconductor Interfaces, Microstructures, and Devices, Properties and Applications*, edited by Feng Z. C. (Institute of Physics Publishing, 1993) pp. 257–270.
15. Soerman E., Son N. T., Chen W. M., Kordina O., Hallin C., Janzen E., *Phys. Rev. B* **61**, 26113 (2000).
16. Singh H., Anisimov A. A., Baranov P. G., Suter D., *arXiv:2212.10256* (2022).
17. Breev I. D., Shang Z., Poshakinskiy A. V., Singh H., Berencén Y., Hollenbach M., Nagalyuk S. S., Mokhov E. N., Babunts R. A., Baranov P. G., Suter D., Tarasenko S. A., Astakhov G. V., Anisimov A. N., *npj Quant. Inform.* **8**, 23 (2022).
18. Biktagirov T., Schmidt W. G., Gerstmann U., Yavkin B., Orlinskii S., Baranov P., Dyakonov V., Soltamov V., *Phys. Rev. B* **98**, 195204 (2018).

19. Soltamov V. A., Soltamova A. A., Baranov P. G., Proskuryakov I. I., *Phys. Rev. Lett.* **108**, 226402 (2012).
20. Van de Stolpe G. L., Kwiatkowski D. P., Bradley C. E., Randall J., Abobeih M. H., Breitweiser S. A., Bassett L. C., Markham M., Twitchen D. J., Taminiau T. H., *Nature Comm.* **15**, 2006 (2024).